

www.acsami.org Research Article

# An Electrochemical Ethylamine/Acetonitrile Redox Method for Ambient Hydrogen Storage

Dezhen Wu, Jialu Li, Libo Yao, Rongxuan Xie, and Zhenmeng Peng\*



Cite This: ACS Appl. Mater. Interfaces 2021, 13, 55292-55298



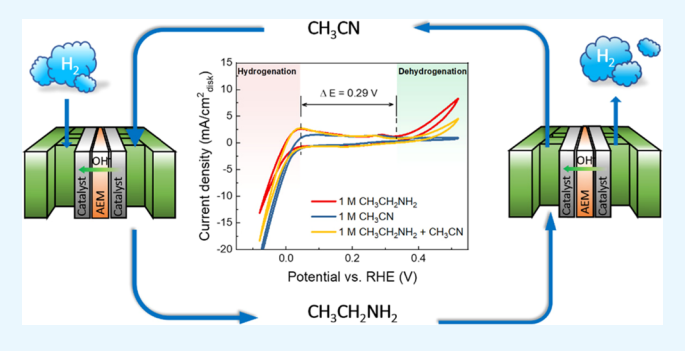
**ACCESS** 

Metrics & More

Article Recommendations

Supporting Information

ABSTRACT: Hydrogen storage presents a major difficulty in the development of hydrogen economy. Herein, we report a new electrochemical ethylamine/acetonitrile redox method for hydrogen storage with an 8.9 wt % theoretical storage capacity under ambient conditions. This method exhibits low onset overpotentials of 0.19 V in CH<sub>3</sub>CH<sub>2</sub>NH<sub>2</sub> dehydrogenation to CH<sub>3</sub>CN and 0.09 V in CH<sub>3</sub>CN hydrogenation to CH<sub>3</sub>CH<sub>2</sub>NH<sub>2</sub> using commercial Pt black catalyst. By assembling a full cell that couples CH<sub>3</sub>CH<sub>2</sub>NH<sub>2</sub>/CH<sub>3</sub>CN redox reactions with hydrogen evolution and oxidation reactions, we demonstrate a complete hydrogen storage cycle at fast rates, with only 52.5 kJ/mol energy consumption for H<sub>2</sub> uptake and release at a rate of 1 L/m<sup>2</sup>·h. This method provides a



viable hydrogen storage strategy that meets the 2025 Department of Energy onboard hydrogen storage target.

KEYWORDS: ambient hydrogen storage, electrocatalytic ethylamine dehydrogenation, electrocatalytic acetonitrile hydrogenation, hydrogen uptake and release, efficiency

# 1. INTRODUCTION

Hydrogen is an appealing energy carrier that can potentially replace conventional fossil fuels in the development of a clean, sustainable hydrogen economy, which would resolve environmental problems caused by the combustion of nonrenewable resources while also meeting the increasing demand for energy. 1,2 However, hydrogen storage has remained a major roadblock in the hydrogen economy development. Currently, hydrogen is mainly stored in the form of either compressed gas or cryogenic liquid. These methods are ill-suited for commercial applications because of their insufficient energy storage density.3 To make matters worse, extreme storage conditions are required, which not only result in a significant increment in cost but also raise safety concerns. As a matter of fact, the state-of-the-art methods fall short of the 2025 Department of Energy (DOE) onboard hydrogen storage target of 5.5 wt % under 85 °C and 12 bar.

To overcome these challenges, there have been extensive research efforts to discover alternative hydrogen storage methods in the past few decades. The developed methods can be primarily classified into two categories, that is, physisorption and chemical conversion, depending on the storage mechanisms. The physisorption methods use large-surface, light-weight storage materials, which can weakly adsorb hydrogen molecules to their surface via the van der Waals attraction force.<sup>3</sup> Although many promising materials have been carefully investigated, such as carbon nanotubes, 4,5 zeolites, 6,7 metal—organic frameworks (MOFs), 8,9 and covalent

organic frameworks (COFs), 10 only a relatively low storage capacity (typically less than 1-2 wt %) can be obtained, even under their best preformed low-temperature and high-pressure conditions.11 Chemical conversion methods involve the uptake of hydrogen by storage materials via hydrogenation and release of hydrogen via decomposition. A range of chemical compounds, for instance, aluminum and magnesium hydrides, 12,13 metal complex hydrides, 14 and amides/imides, 15 have been considered as promising candidates and extensively studied. Many of these chemical compounds possess >5.5 wt % theoretical hydrogen uptake/release that exceeds the DOE goal of storage capacity. However, to date, none of them have been able to meet the DOE goals regarding operation conditions and cost. This is because these chemical hydrogen storage processes generally go through complex reaction pathways with a high energy barrier. Furthermore, either the hydrogen uptake or release reaction would be endothermic from a thermodynamics point of view. Extremely high temperature and pressure conditions were thus required to complete a hydrogen storage cycle in these previous studies.<sup>3</sup>

Received: October 23, 2021 Accepted: November 4, 2021 Published: November 15, 2021





In this work, we report a new, electrochemical ethylamine/ acetonitrile redox method for efficient, high-capacity hydrogen storage under completely ambient conditions. The amine/ nitrile redox couple is selected because of its moderate chemical polarity and relatively simple hydrogenation and dehydrogenation pathways, which would aid reaction activation and reduce the energy barrier. Electrochemical potential provides the driving force in CH<sub>3</sub>CH<sub>2</sub>NH<sub>2</sub> dehydrogenation under ambient conditions, rather than high temperature and pressure that are typically required to thermally drive an endothermic process. We demonstrate an effective, complete cycle of CH<sub>3</sub>CN hydrogenation to CH<sub>3</sub>CH<sub>2</sub>NH<sub>2</sub> for hydrogen uptake and CH3CH2NH2 dehydrogenation to CH3CN for hydrogen release at low overpotentials, using commercial Pt black catalyst in an electrochemical cell. The studied CH<sub>3</sub>CH<sub>2</sub>NH<sub>2</sub>/CH<sub>3</sub>CN system has a theoretical H<sub>2</sub> storage capacity of 8.9 wt %, well surpassing the 5.5 wt % DOE target. This study offers a new, effective hydrogen storage strategy that can be extended to many other amine/nitrile redox systems and would help advance the hydrogen economy development.

# 2. EXPERIMENTAL SECTION

2.1. Materials. Commercial platinum black (high surface area, 45-52 m<sup>2</sup>/g), fumasep FAB-PK-130 (anion-exchange membrane), sigracet 22 BB (carbon paper) were purchased from Fuel Cell Store. Ethylamine solution (CH<sub>3</sub>CH<sub>2</sub>NH<sub>2</sub>, 66.0-72.0% in H<sub>2</sub>O) and sodium hydroxide (NaOH, ACS reagent, ≥ 97%) were purchased from Sigma-Aldrich. Acetonitrile (CH<sub>3</sub>CN, HiPerSolv, ≥97%) was purchased from VWR.

2.2. Half-Cell Working Electrode Preparation. A solution was prepared by mixing isopropanol with Nafion ionomer with a volume ratio of  $V_{\text{isopropanol}}$ :  $V_{\text{Nafion}} = 250:1$ . The catalyst ink was obtained by dispersing 4 mg of commercial Pt black catalyst into 4 mL of the prepared solution (1 mg of catalyst/mL of solution). Then, the catalyst ink was sonicated for 15-30 min until a good dispersion was obtained. After that, 25 µL of catalyst ink was transferred dropwise onto a clean glassy carbon rotating disk electrode (RDE, 5 mm in diameter). There was an interval of 5 min between drops to ensure complete solvent evaporation to obtain a homogeneous catalyst film. The final catalyst loading was 127.6  $\mu g_{Pt}/cm^2$ .

2.3. Electrochemical Measurements under Half-Cell Conditions. A three-electrode system was used to perform electrochemical measurements of all half-cell reactions on a CHI 760D electrochemical workstation (CH Instruments, Inc.). The working electrode was a catalyst-coated rotating disk electrode. The counter electrode was a Pt wire. The reference electrode was an Ag/AgCl electrode (CH Instruments, Inc.). In a typical ethylamine dehydrogenation reaction, the electrolyte was an aqueous solution containing 1 M CH<sub>3</sub>CH<sub>2</sub>NH<sub>2</sub> and 1 M NaOH. The electrolyte was purged using argon for 20 min before any measurement to remove trace amounts of dissolved air. After that, because of the low boiling point of ethylamine (16.6 °C), the electrochemical cell was sealed completely to prevent vapors from escaping the system. Cyclic voltammetry (CV) was performed at a scanning rate of 50 mV/s. Linear sweep voltammetry (LSV) was conducted at a scanning rate of 10 mV/s. The liquid product was collected immediately after the reaction for nuclear magnetic resonance (NMR) characterizations. In a typical acetonitrile hydrogenation reaction, the electrolyte was an aqueous solution containing 1 M CH<sub>3</sub>CN and 1 M NaOH. The electrolyte was saturated with hydrogen to enable hydrogen oxidation reaction (HOR). The rest of the experiments was conducted in the same manner. The electrochemical tests at different temperatures were conducted by immersing the sealed electrochemical cell into an ice bath, and the temperature was controlled between 0 and 20 °C. All potentials were calibrated, converted, and presented relative to the reversible hydrogen electrode (RHE) in this article, if not specified

otherwise, using the following equation: E (vs RHE) = E (vs Ag/ AgCl) + 0.197 V + 0.059  $\times$  pH. All experiments were carried out in a similar manner with independent variables, such as the solvent concentration, pH value, and temperature, which were specified in the

2.4. Electrochemical Measurements in Full-Cell Mode. A homemade 3.2 cm × 3.2 cm anion-exchange membrane (AEM) full cell was assembled and used for hydrogen uptake and release tests. The membrane electrode assembly (MEA) used during the experiments consisted of a Pt anode, a PK reinforced AEM (fuel cell store), and a Pt cathode. The AEM was treated with 1.0 M KOH solution to remove possible additives prior to use. To prepare both anode and cathode inks, the commercial Pt black catalyst was mixed with an anion-exchange ionomer (polyaromatic polymer) with the ratio of 80:30 in the dimethylformamide (DMF) solvent. The inks were sonicated for 30 min to prepare a good dispersion. Then, they were drop-cast onto gas diffusion layers with an area of 10 cm<sup>2</sup> (5% polytetrafluoroethylene-treated carbon paper for gas diffusion and hydrophilic carbon cloth for liquid diffusion). The metal loading on both layers was 1 mg<sub>Pt</sub>/cm<sup>2</sup>. Finally, the pretreated membrane and electrodes with an area of 10 cm<sup>2</sup> were bonded together using the hotpressing method.

The tests for hydrogen release [i.e., ethylamine dehydrogenation reaction coupled with hydrogen evolution reaction (HER)] were performed at room temperature under a N<sub>2</sub> gas flow of 100 mL/min on the cathode and an aqueous electrolyte (2 M ethylamine, 0.5 M NaOH) flow of 5 mL/min on the anode. The tests for hydrogen uptake (i.e., acetonitrile hydrogenation reaction coupled with HOR) were performed at room temperature under a H<sub>2</sub> gas flow of 100 mL/ min on the anode and an aqueous electrolyte (2 M acetonitrile, 0.5 M NaOH) flow of 5 mL/min on the cathode.

2.5. Product Characterizations and Quantifications. NMR was carried out on a research-grade 750 MHz Varian INOVA instrument. On-line mass spectrometry (MS) was conducted on a UGA Series Universal Gas Analyzer.

We used <sup>1</sup>H-NMR to quantify the amounts of liquid products from acetonitrile hydrogenation in hydrogen uptake experiments, with acetonitrile as the internal standard. The NMR samples were prepared in a mixture of D2O and collected liquid reaction products with a volume ratio of 80%:20%.

MS was used to quantify the amount of hydrogen generated during ethylamine dehydrogenation in hydrogen release experiments. For online MS quantification, a calibration curve was plotted regarding the relationship between the hydrogen partial pressure (x) and change in hydrogen signal intensity (y) in MS, which was determined as follows:

$$y = 711.5x - 0.1378\tag{1}$$

Then, instantaneous hydrogen generation rate (molar flow rate) was calculated using the following equation:

$$\dot{n} = \frac{P_{\rm H2} \times \dot{V}}{RT} \tag{2}$$

Here,  $P_{\rm H2}$  is the hydrogen partial pressure.  $\dot{V}$  is the gas volumetric flow rate. R is the ideal gas constant. T is temperature.

The Faradaic efficiency (FE) was calculated based on the following

$$FE (\%) = \frac{NF \int \dot{n} dt}{Q} \tag{3}$$

Here, N is the electron needed in the reaction to produce one hydrogen molecule. F is Faraday's constant.  $\dot{n}$  is the hydrogen molar flow rate. Q is the total charge transfer.

# 3. RESULTS AND DISCUSSION

The electrochemical conversion between CH<sub>3</sub>CH<sub>2</sub>NH<sub>2</sub> and CH<sub>3</sub>CN in an alkaline aqueous electrolyte occurs via a fourelectron transfer dehydrogenation/hydrogenation process and exhibits a standard redox potential of 0.13 V vs RHE (Figure

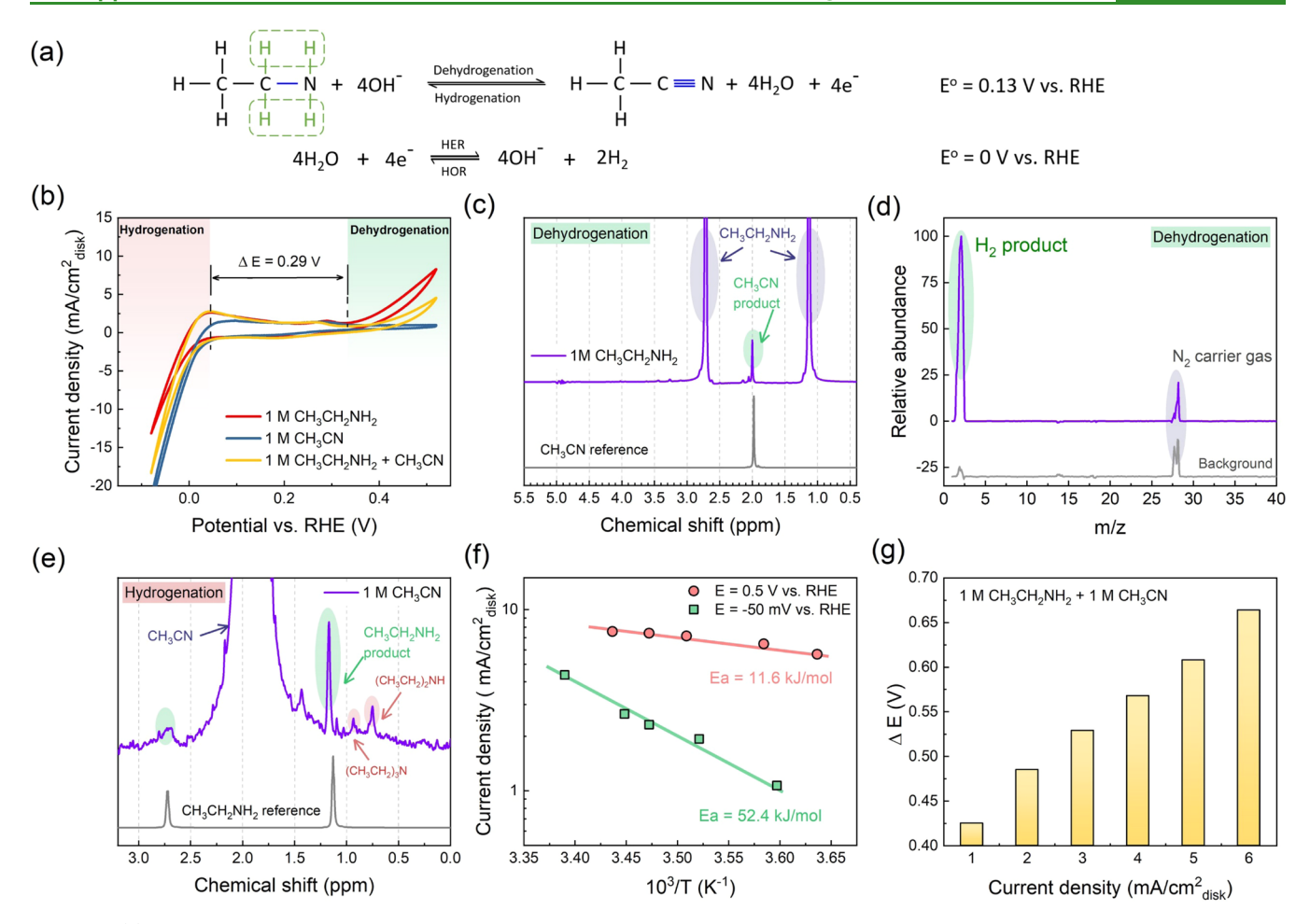


Figure 1. (a) Equation and standard potential for electrochemical  $CH_3CH_2NH_2/CH_3CN$  redox reactions and hydrogen evolution and oxidation reactions under alkaline aqueous conditions; (b) CV of commercial Pt black catalyst-loaded working electrode in 1 M NaOH aqueous solution with the addition of 1 M  $CH_3CH_2NH_2$ , 1 M  $CH_3CN$ , and 1 M  $CH_3CH_2NH_2$  + 1 M  $CH_3CN$ ; (c) <sup>1</sup>H NMR spectrum of the liquid product from  $CH_3CH_2NH_2$  dehydrogenation obtained by applying 0.7 V vs RHE for 10 h, with  $CH_3CN$  as a reference and (d) mass spectrum of the gas product from the counter electrode in the  $CH_3CH_2NH_2$  dehydrogenation experiment; (e) <sup>1</sup>H NMR spectrum of the liquid product from  $CH_3CN$  hydrogenation obtained by applying -0.4 V vs RHE for 10 h, with  $CH_3CH_2NH_2$  as a reference; (f) Arrhenius plots obtained at 0.5 V vs RHE in  $CH_3CH_2NH_2$  dehydrogenation experiments and at -50 mV vs RHE in  $CH_3CN$  hydrogenation experiments; (g) potential difference between  $CH_3CH_2NH_2$  dehydrogenation reaction and  $CH_3CN$  hydrogenation reaction of current density in 1 M NaOH aqueous solution with the addition of 1 M  $CH_3CH_2NH_2$  and 1 M  $CH_3CN$ .

1a). The reaction properties were studied by conducting electrochemical measurements under half-cell test conditions, with the working electrode loaded with the commercial Pt black catalyst for promoting the kinetics. Figure 1b and S1 show CV and LSV data collected in different electrolytes. In a 1 M CH<sub>3</sub>CH<sub>2</sub>NH<sub>2</sub> + 1 M NaOH electrolyte, the CV curve exhibited cathodic currents below 0 V, which corresponded to HER, and anodic currents above 0.32 V, which was attributed to CH<sub>3</sub>CH<sub>2</sub>NH<sub>2</sub> electrochemical oxidation because the anodic currents became negligible with the absence of CH<sub>3</sub>CH<sub>2</sub>NH<sub>2</sub> in the electrolyte. Proton nuclear magnetic resonance (1H NMR) spectroscopy characterizations of the reacted solution found CH<sub>3</sub>CN to be the only liquid product (Figure 1c), confirming effective, selective CH<sub>3</sub>CH<sub>2</sub>NH<sub>2</sub> dehydrogenation to CH<sub>3</sub>CN. The measured low onset overpotential of about 0.19 V suggested fast dehydrogenation kinetics. This could benefit from a moderate polarity and basicity of amine molecules, which would allow for efficient activation toward electrochemical oxidation. 16,17 The occurrence of CH<sub>3</sub>CH<sub>2</sub>NH<sub>2</sub> dehydrogenation on the working electrode was accompanied by HER on the counter electrode, as evidenced

by MS detection of the  $H_2$  product in the gas phase (Figure 1d).

With the addition of CH<sub>3</sub>CN to the electrolyte, the CV curve showed more significant cathodic currents below 0 V vs RHE. Moreover, there was a slight positive shift in the onset potential to 0.04 V. These results suggested the occurrence of CH<sub>3</sub>CN electrochemistry with an onset overpotential of 0.09 V, in addition to HER. The <sup>1</sup>H NMR spectrum of the reaction product showed CH<sub>3</sub>CH<sub>2</sub>NH<sub>2</sub> as a major product and minor fractions of (CH<sub>3</sub>CH<sub>2</sub>)<sub>2</sub>NH and (CH<sub>3</sub>CH<sub>2</sub>)<sub>3</sub>N side products (Figure 1e). 18,19 This confirmed that CH<sub>3</sub>CN can be effectively converted to CH<sub>3</sub>CH<sub>2</sub>NH<sub>2</sub> via electrochemical hydrogenation. It is worth noting that the CH<sub>3</sub>CN hydrogenation efficiency and selectivity can be further improved by catalyst research. For instance, Zhang et al. reported complete prevention of amine dimer and trimer formation and suppression of HER in CH3CN hydrogenation to CH<sub>3</sub>CH<sub>2</sub>NH<sub>2</sub> using a Cu catalyst. 19 Xia et al. investigated several catalyst materials in CH<sub>3</sub>CN hydrogenation and found composition effects on the reaction activity and selectivity properties. 18

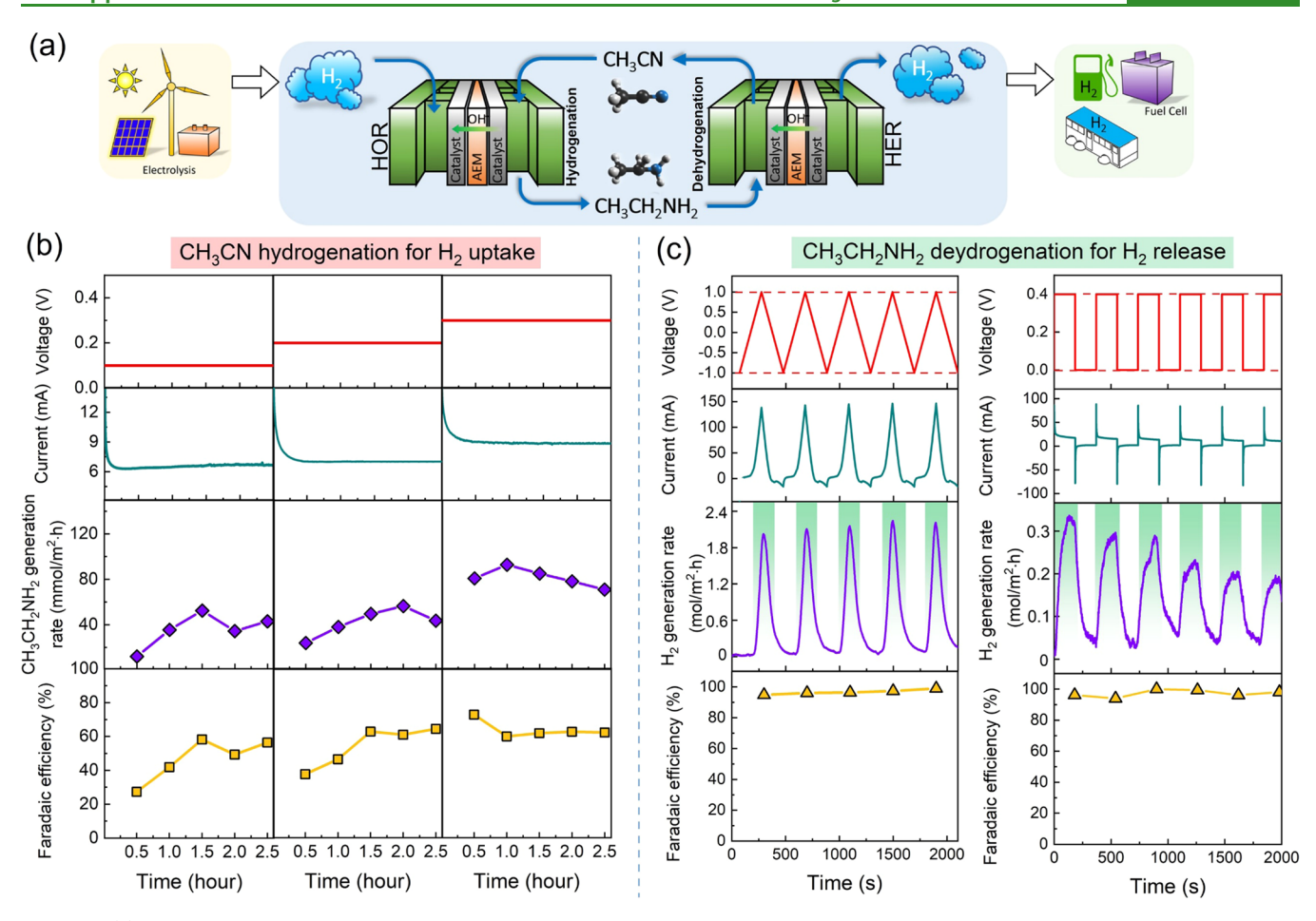


Figure 2. (a) Schematic drawing of a full-cell system that realizes a complete cycle of hydrogen storage under ambient conditions by coupling the electrochemical CH<sub>3</sub>CH<sub>2</sub>NH<sub>2</sub>/CH<sub>3</sub>CN redox method with HER/HOR, with hydrogen production from renewable energy and hydrogen applications included to illustrate the sustainable hydrogen economy; (b) chronoamperometry of CH<sub>3</sub>CN hydrogenation for H<sub>2</sub> uptake at different cell voltages, and the measured CH<sub>3</sub>CH<sub>2</sub>NH<sub>2</sub> generation rate and FE; (c) CV and on-and-off chronoamperometry of CH<sub>3</sub>CH<sub>2</sub>NH<sub>2</sub> dehydrogenation for H<sub>2</sub> release, and the measured H<sub>2</sub> generation rate and FE under the testing conditions.

The effects of electrolyte pH and concentration on both CH<sub>3</sub>CH<sub>2</sub>NH<sub>2</sub> dehydrogenation and CH<sub>3</sub>CN hydrogenation reaction properties were investigated. The highest current density for CH<sub>3</sub>CH<sub>2</sub>NH<sub>2</sub> dehydrogenation was obtained with 0.5 M NaOH, suggesting the optimal pH for this reaction (Figure S2 and S3). With an increase in the CH<sub>3</sub>CH<sub>2</sub>NH<sub>2</sub> concentration, there was an improvement in the dehydrogenation rate together with suppression in HER (Figure S4-S6). This can be explained by the strong adsorption of amino groups to the Pt catalyst, 16,17 with which a higher concentration of CH<sub>3</sub>CH<sub>2</sub>NH<sub>2</sub> would lead to more active sites being occupied for its dehydrogenation and less active sites for HER. Chronoamperometry experiments at 0.5 V vs RHE show time dependency of the current density (Figure S7), which had a drastic decrease at the beginning and became more stabilized thereafter. The negligible influence of the electrode rotation rate on CH3CH2NH2 dehydrogenation indicated minimal mass-transfer limitation for this reaction under the studied condition (Figure S8). For the reverse CH<sub>3</sub>CN hydrogenation reaction, a higher current density was obtained with an increase in the pH and a decrease in the CH<sub>3</sub>CN concentration (Figure S9 and S10). Because CH<sub>3</sub>CN hydrogenation and HER occur simultaneously in the same potential region, there would be an interplay between the two processes that lead to the observed changes. While the

electrode rotation rate did not show a significant effect on the current density in the  $\mathrm{CH_3CN}$  hydrogenation region, it considerably affected the current density in the positive potential range that corresponded to HOR, particularly when the electrolyte was saturated with  $\mathrm{H_2}$  (Figure S11). This was consistent with previous HOR studies and was attributed to a mass-transfer limitation in this reaction.

The temperature effect on the two half-cell reactions was studied by measuring the LSV change with temperature, which was used for evaluating the reaction activity property (Figure S12 and S13). Figure 1f shows the obtained Arrhenius plot, which determined an apparent activation energy  $(E_a)$  value of 52.4 kJ/mol at 0.5 V vs RHE for CH<sub>3</sub>CH<sub>2</sub>NH<sub>2</sub> dehydrogenation and 11.6 kJ/mol at -0.05 V vs RHE. Although the latter accounted for CH3CN hydrogenation with a mix of HER, these low  $E_a$  values revealed the rapid reaction kinetics and agreed well with the observed low overpotentials in CH<sub>3</sub>CH<sub>2</sub>NH<sub>2</sub> dehydrogenation and CH<sub>3</sub>CN hydrogenation. Benefiting from their low activation energy, a minimal increase in the potential difference between the two half-cell reactions is needed to drastically improve the reaction current density (Figure 1g), implying the feasibility of utilizing these two reactions to realize energy-efficient, complete cycle of hydrogen storage.

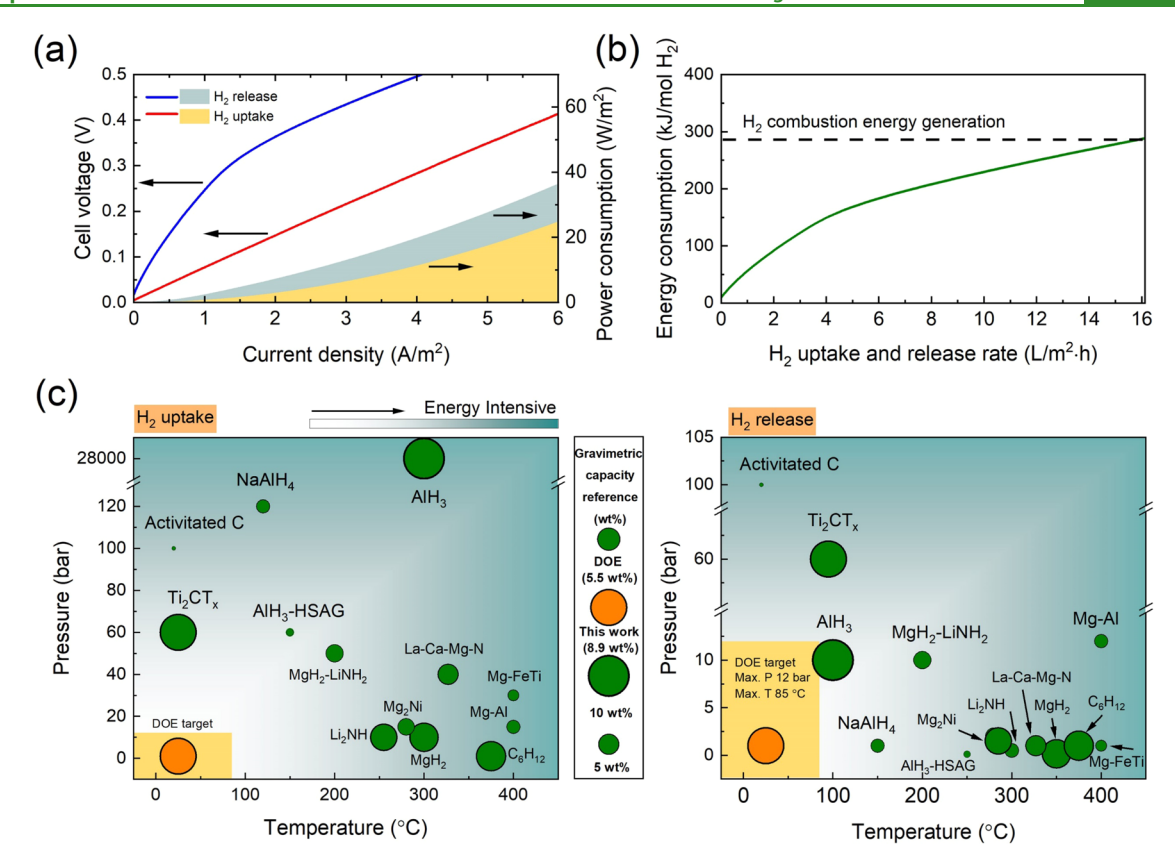


Figure 3. (a) Full-cell I–V curves for H<sub>2</sub> uptake and release steps, and corresponding power consumption; (b) calculated energy consumption for completing a complete hydrogen storage cycle as a function of H<sub>2</sub> uptake and release rate; (c) comparison of the electrochemical CH<sub>3</sub>CH<sub>2</sub>NH<sub>2</sub>/CH<sub>3</sub>CN redox method with literature data of other reported methods in terms of hydrogen storage capacity, operation pressure, and temperature.

Figure 2a illustrated the blueprint for a sustainable hydrogen economy, in which the electrochemical CH<sub>3</sub>CH<sub>2</sub>NH<sub>2</sub>/CH<sub>3</sub>CN redox method plays a crucial role for hydrogen storage that bridges hydrogen production and various applications. The great potential of this new method was demonstrated by assembling a custom-made 10 cm<sup>2</sup> electrochemical cell and investigating the overall hydrogenation/dehydrogenation process to simulate a complete H<sub>2</sub> uptake/release cycle (Figure S14). In H<sub>2</sub> uptake experiments, CH<sub>3</sub>CN and H<sub>2</sub> were fed to the cathode and anode, at which CH<sub>3</sub>CN hydrogenation and HOR occurred with an applied cell voltage (Figure S15). Figure 2b shows chronoamperometry tests of the cell at different voltages and the corresponding H2 uptake performances. A notable current was measured even with a low cell voltage of 0.1 V. Except for the initial drop due to the capacitive current effect, the cell maintained a consistent current of roughly 6 mA throughout the experiment, indicating good durability for CH3CN hydrogenation and HOR reactions. An increase in the cell voltage led to enhancements in the H2 uptake rate. This was evidenced by the measured current and the CH<sub>3</sub>CH<sub>2</sub>NH<sub>2</sub> generation rate quantified with NMR analysis (Figure S16), with CH<sub>3</sub>CH<sub>2</sub>NH<sub>2</sub> being produced at as high as 93.1 mmol/m<sup>2</sup>·h rate at 0.3 V. With increasing cell voltage, the FE for CH<sub>3</sub>CH<sub>2</sub>NH<sub>2</sub> production gradually increased, reaching about 60% at 0.3 V. The nonsuperior CH<sub>3</sub>CH<sub>2</sub>NH<sub>2</sub> FE was obtained by side reactions including HER and the generation of (CH3CH2)2NH and (CH<sub>3</sub>CH<sub>2</sub>)<sub>3</sub>N minor products, which was in agreement with the results under half-cell conditions and can be improved by applying a more suitable catalyst. <sup>18,19</sup> For H<sub>2</sub> release, CH<sub>3</sub>CH<sub>2</sub>NH<sub>2</sub> was fed to the anode and dehydrogenated to

CH<sub>3</sub>CN with an applied cell voltage (Figure S17). This was coupled with HER at the cathode, transforming the hydrogen stored in the CH<sub>3</sub>CH<sub>2</sub>NH<sub>2</sub> molecules to H<sub>2</sub> gas. Figure 2c shows CV and chronoamperometry results of the cell, with H<sub>2</sub> generation being continuously measured using on-line MS (Figure S18-S19). The H<sub>2</sub> generation became significant once the cell voltage turned positive, with the generation rate increasing rapidly with the voltage and the FE determined to be close to 100%. This was consistent with the finding of CH<sub>3</sub>CN as the only liquid product and H<sub>2</sub> as the only gas product, confirming an excellent selectivity in H2 release via CH<sub>3</sub>CH<sub>2</sub>NH<sub>2</sub> dehydrogenation. The cell durability was evaluated by conducting chronoamperometry experiments at different voltages. The current showed a rapid drop in the first few minutes and then became steadier throughout the remaining experiment with a constant voltage being applied (Figure S20), suggesting promising cell durability. The current decayed more rapidly when the voltage was periodically turned on and off for simulating cell startup and shutdown operations (Figure 2c), and the decay became more substantial as the voltage increased (Figure S21 and S22). This was likely due to a gradual deactivation of the Pt black catalyst under these stability test conditions. Regardless of the cell voltage, the FE was consistently greater than 94% and exhibited no signs of decrease.

We conducted an energy consumption analysis using the cell LSV data to assess the technical feasibility of this new electrochemical  $CH_3CH_2NH_2/$   $CH_3CN$  redox method for hydrogen storage applications. Figure 3a shows the measured cell I–V plots during  $H_2$  uptake and release processes as well as the calculated power consumption in the individual steps,

based on which the total energy consumption to complete a hydrogen storage cycle at any designated hydrogen uptake and release rate was computed (Figure 3b). It appeared that the energy consumption per mole of H<sub>2</sub> for a complete storage cycle was a function of H<sub>2</sub> uptake and release rate, with extremely low energy consumption at slow rates. For instance, the  $H_2$  uptake and release at a rate of 1 L/m<sup>2</sup>·h required only 52.5 kJ/mol energy consumption, which was dramatically smaller compared to 286 kJ/mol energy generation when the stored H2 is combusted for application, suggesting the energyefficient nature of the electrochemical CH<sub>3</sub>CH<sub>2</sub>NH<sub>2</sub>/CH<sub>3</sub>CN redox method. Additionally, the uptake/release temperature and pressure conditions should also be taken into account for cost and safety concerns. Although certain metal hydrides can achieve a high storage capacity, for instance, 7 wt % for  $MgH_2$  and 10 wt % for  $AlH_3$ , their hydrogen uptake/release process requires either >300 °C temperature or > 20 bar pressure, if not both (Figure 3c). A very recent study by Liu et al. reported a new multilayered Ti<sub>2</sub>CT<sub>x</sub> material with 8.8 wt % storage capacity at 60 bar, but achieved only 4 wt % under ambient conditions.<sup>26</sup> It is unprecedented that the electrochemical CH<sub>3</sub>CH<sub>2</sub>NH<sub>2</sub>/CH<sub>3</sub>CN redox method is capable of completing a hydrogen uptake and release cycle with 8.9 wt % storage capacity under entirely ambient conditions. To the best of our knowledge, this new method is the only approach that meets the 2025 DOE onboard hydrogen storage target in terms of storage capacity (≥5.5 wt %), max delivery temperature ( $\leq 85$  °C), and max delivery pressure ( $\leq 12$  bar).

# 4. CONCLUSIONS

In summary, a novel electrochemical CH<sub>3</sub>CH<sub>2</sub>NH<sub>2</sub>/CH<sub>3</sub>CN redox method was studied for ambient H2 storage, which utilized electrochemical conversion between the two chemicals. CH<sub>3</sub>CH<sub>2</sub>NH<sub>2</sub> dehydrogenation to CH<sub>3</sub>CN using a commercial Pt black catalyst exhibited a low onset overpotential of 0.19 V and a moderate activation energy of 52.4 kJ/mol at 0.5 V vs RHE and produced CH<sub>3</sub>CN as the only product, indicating fast reaction kinetics and excellent selectivity. The rapid CH<sub>3</sub>CN hydrogenation to CH<sub>3</sub>CH<sub>2</sub>NH<sub>2</sub> was also evidenced by a low onset overpotential of 0.09 V and a low activation energy of 11.6 kJ/mol. A complete hydrogen uptake and release cycle was demonstrated with full-cell testing, with 93.14 mmol/m<sup>2</sup>·h CH<sub>3</sub>CH<sub>2</sub>NH<sub>2</sub> generation rate and 60% FE for H<sub>2</sub> uptake at 0.3 V cell voltage, and 0.34 mol/m<sup>2</sup>·h H<sub>2</sub> generation rate and > 94% FE for H<sub>2</sub> release at 0.4 V cell voltage. It is worth mentioning that these results were obtained in a simply assembled electrochemical cell using commercial Pt black catalyst, implying the H<sub>2</sub> uptake and release rate, as well as the FE can be further improved with cell engineering and new catalyst research. With 8.9 wt % theoretical H<sub>2</sub> storage capacity, ambient reaction conditions, and 52.5 kJ/mol low energy consumption for H2 uptake and release at a rate of 1 L/ m<sup>2</sup>·h, this study demonstrated the CH<sub>3</sub>CH<sub>2</sub>NH<sub>2</sub>/CH<sub>3</sub>CN redox method as a viable hydrogen storage strategy that would contribute to advancing the hydrogen economy development.

# ■ ASSOCIATED CONTENT

#### **Supporting Information**

The Supporting Information is available free of charge at https://pubs.acs.org/doi/10.1021/acsami.1c20498.

CV curves; polarization curves and chronoamperometric i-t curves using Pt black catalyst in aqueous solution for

electrochemical dehydrogenation of ethylamine and hydrogenation of acetonitrile under different conditions, including various pH values, concentrations of reactants, and reaction temperatures; photographs of the assembled electrochemical cell; NMR spectra of the collected liquid aliquot from the full-cell hydrogen uptake experiment; CV curve and polarization curve obtained in an electrochemical full cell and the representative MS spectra of the gas product on the cathode in the full-cell hydrogen release experiment; and on-and-off chronoamperometry of CH<sub>3</sub>CH<sub>2</sub>NH<sub>2</sub> dehydrogenation for H<sub>2</sub> release. (PDF)

# AUTHOR INFORMATION

#### **Corresponding Author**

Zhenmeng Peng — Department of Chemical, Biomolecular, and Corrosion Engineering, The University of Akron, Akron, Ohio 44325, United States; orcid.org/0000-0003-1230-6800; Email: zpeng@uakron.edu

#### **Authors**

**Dezhen Wu** – Department of Chemical, Biomolecular, and Corrosion Engineering, The University of Akron, Akron, Ohio 44325, United States

Jialu Li – Department of Chemical, Biomolecular, and Corrosion Engineering, The University of Akron, Akron, Ohio 44325, United States

Libo Yao — Department of Chemical, Biomolecular, and Corrosion Engineering, The University of Akron, Akron, Ohio 44325, United States

Rongxuan Xie – Department of Chemical, Biomolecular, and Corrosion Engineering, The University of Akron, Akron, Ohio 44325, United States

Complete contact information is available at: https://pubs.acs.org/10.1021/acsami.1c20498

#### **Author Contributions**

D.Z.W. and J.L.L. contributed equally to this work. D.Z.W. designed and performed the half-cell experiments, analyzed the data, and prepared the manuscript. J.L.L. conducted the full cell assembling, calibration and testing, and characterization of the reaction products. L.B.Y. and R.X.X. contributed to full-cell assembling and testing and result discussion. Z.M.P. conceived the project, designed the experiments, and edited the manuscript.

#### **Funding**

The University of Akron, US. National Science Foundation (NSF) 1,955,452.

#### **Notes**

The authors declare no competing financial interest.

# ACKNOWLEDGMENTS

The authors appreciate the financial support from The University of Akron and National Science Foundation.

### REFERENCES

- (1) Crabtree, G. W.; Dresselhaus, M. S.; Buchanan, M. V. The Hydrogen Economy. *Phys. Today* **2004**, *57*, 39–44.
- (2) Penner, S. S. Steps toward the Hydrogen Economy. *Energy* **2006**, 31, 33–43.
- (3) Jena, P. Materials for Hydrogen Storage: Past, Present, and Future. J. Phys. Chem. Lett. 2011, 2, 206–211.

- (4) Dillon, A. C.; Jones, K. M.; Bekkedahl, T. A.; Kiang, C. H.; Bethune, D. S.; Heben, M. J. Storage of Hydrogen in Single-Walled Carbon Nanotubes. *Nature* **1997**, *386*, 377–379.
- (5) Chen, P.; Wu, X.; Lin, J.; Tan, K. L. High H<sub>2</sub> Uptake by Alkali-Doped Carbon Nanotubes under Ambient Pressure and Moderate Temperatures. *Science* **1999**, 285, 91–93.
- (6) Weitkamp, J.; Fritz, M.; Ernst, S. Zeolites as Media for Hydrogen Storage. In *Proceedings from the ninth international zeolite conference*; Elsevier, 1993; 11–19.
- (7) Dong, J.; Wang, X.; Xu, H.; Zhao, Q.; Li, J. Hydrogen Storage in Several Microporous Zeolites. *Int. J. Hydrogen Energy* **2007**, 32, 4998–5004
- (8) Kaye, S. S.; Dailly, A.; Yaghi, O. M.; Long, J. R. Impact of Preparation and Handling on the Hydrogen Storage Properties of Zn<sub>4</sub>O (1, 4-Benzenedicarboxylate) 3 (MOF-5). *J. Am. Chem. Soc.* **2007**, *129*, 14176–14177.
- (9) Yang, J.; Grzech, A.; Mulder, F. M.; Dingemans, T. J. Methyl Modified MOF-5: A Water Stable Hydrogen Storage Material. *Chem. Commun.* **2011**, 47, 5244–5246.
- (10) Ke, Z.; Cheng, Y.; Yang, S.; Li, F.; Ding, L. Modification of COF-108 via Impregnation/Functionalization and Li-Doping for Hydrogen Storage at Ambient Temperature. *International Journal of Hydrogen Energy* **2017**, 42, 11461–11468.
- (11) Niaz, S.; Manzoor, T.; Pandith, A. H. Hydrogen Storage: Materials, Methods and Perspectives. *Renew. Sustain. Energy Rev.* **2015**, *50*, 457–469.
- (12) Jensen, C. M.; Gross, K. J. Development of Catalytically Enhanced Sodium Aluminum Hydride as a Hydrogen-Storage Material. *Appl. Phys. A: Mater. Sci. Process.* **2001**, 72, 213–219.
- (13) de Rango, P.; Marty, P.; Fruchart, D. Hydrogen Storage Systems Based on Magnesium Hydride: From Laboratory Tests to Fuel Cell Integration. *Appl. Phys. A* **2016**, *122*, 1–20.
- (14) Ley, M. B.; Jepsen, L. H.; Lee, Y.-S.; Cho, Y. W.; Von Colbe, J. M. B.; Dornheim, M.; Rokni, M.; Jensen, J. O.; Sloth, M.; Filinchuk, Y. Complex Hydrides for Hydrogen Storage—New Perspectives. *Mater. Today* **2014**, *17*, 122—128.
- (15) David, W. I. F.; Jones, M. O.; Gregory, D. H.; Jewell, C. M.; Johnson, S. R.; Walton, A.; Edwards, P. P. A Mechanism for Non-Stoichiometry in the Lithium Amide/Lithium Imide Hydrogen Storage Reaction. *J. Am. Chem. Soc.* **2007**, *129*, 1594–1601.
- (16) Adenier, A.; Chehimi, M. M.; Gallardo, I.; Pinson, J.; Vilà, N. Electrochemical Oxidation of Aliphatic Amines and Their Attachment to Carbon and Metal Surfaces. *Langmuir* **2004**, *20*, 8243–8253.
- (17) Ghilane, J.; Martin, P.; Randriamahazaka, H.; Lacroix, J. C. Electrochemical Oxidation of Primary Amine in Ionic Liquid Media: Formation of Organic Layer Attached to Electrode Surface. *Electrochem. Commun.* **2010**, *12*, 246–249.
- (18) Xia, R.; Tian, D.; Kattel, S.; Hasa, B.; Shin, H.; Ma, X.; Chen, J. G.; Jiao, F. Electrochemical Reduction of Acetonitrile to Ethylamine. *Nat. Commun.* **2021**, *12*, 1–8.
- (19) Zhang, D.; Chen, J.; Hao, Z.; Jiao, L.; Ge, Q.; Fu, W.-F.; Lv, X.-J. Highly Efficient Electrochemical Hydrogenation of Acetonitrile to Ethylamine for Primary Amine Synthesis and Promising Hydrogen Storage. *Chem. Catal.* **2021**, 393–406.
- (20) Scofield, M. E.; Zhou, Y.; Yue, S.; Wang, L.; Su, D.; Tong, X.; Vukmirovic, M. B.; Adzic, R. R.; Wong, S. S. Role of Chemical Composition in the Enhanced Catalytic Activity of Pt-Based Alloyed Ultrathin Nanowires for the Hydrogen Oxidation Reaction under Alkaline Conditions. ACS Catal. 2016, 6, 3895–3908.
- (21) Huot, J.; Liang, G.; Boily, S.; Van Neste, A.; Schulz, R. Structural Study and Hydrogen Sorption Kinetics of Ball-Milled Magnesium Hydride. *J. Alloys Compd.* **1999**, 293-295, 495–500.
- (22) Wang, L.; Rawal, A.; Aguey-Zinsou, K.-F. Hydrogen Storage Properties of Nanoconfined Aluminium Hydride (AlH3). *Chem. Eng. Sci.* **2019**, *194*, 64–70.
- (23) Graetz, J.; Hauback, B. C. Recent Developments in Aluminum-Based Hydrides for Hydrogen Storage. MRS Bull. 2013, 38, 473–479.

- (24) Chen, Y.; Wu, C.-Z.; Wang, P.; Cheng, H.-M. Structure and Hydrogen Storage Property of Ball-Milled LiNH<sub>2</sub>/MgH<sub>2</sub> Mixture. *Int. J. Hydrogen Energy* **2006**, *31*, 1236–1240.
- (25) Xiong, Z.; Wu, G.; Hu, J.; Chen, P. Ternary Imides for Hydrogen Storage. Adv. Mater. 2004, 16, 1522-1525.
- (26) Liu, S.; Liu, J.; Liu, X.; Shang, J.; Xu, L.; Yu, R.; Shui, J. Hydrogen Storage in Incompletely Etched Multilayer Ti<sub>2</sub>CT<sub>x</sub> at Room Temperature. *Nat. Nanotechnol.* **2021**, *16*, 331–336.